2005

þÿ An ocean model s response to scatterometer winds

Tokmakian, R.

Ocean Modeling, Volume 9, pp. 89-103, 2005.
http://hdl.handle.net/10945/43117

Available online at www.sciencedirect.com
SCIENCE DIRECT®
Ocean Modelling 9 (2005) 89–103
Ocean Modelling
www.elsevier.com/locate/ocemod

An ocean model's response to scatterometer winds

R. Tokmakian *

Department of Oceanography, Naval Postgraduate School, 833 Dyer Road, Building 232, Rm 328, Monterey, CA 93943, USA

Received 22 March 2004; received in revised form 23 March 2004; accepted 21 April 2004
Available online 8 May 2004

Abstract

Two simulations of the North Atlantic have been run using the POP ocean model for approximately two and one half years each. One simulation used the 1.25° wind product from ECMWF and the other used the JPL Quikscat 0.25° gridded product. The resulting sea level anomaly fields from the simulations are quantified by using tide gauge and altimetric sea level anomaly data. In addition, upper ocean quantities were compared, such as the mix layer depths, to understand the difference in the ocean's response when using the different wind products. The analysis found that significant improvements were made in the representation at the surface, and in particular areas where comparison data exists such as the Labrador Sea. There was also improvement in the scatterometer forced run with more realistic depths of the mixed layer.

Keywords: North Atlantic; Modeling; Scatterometry; Altimetry; Sea level; Upper ocean processes

1. Introduction

Several sets of gridded scatterometer fields have been made available for use in forcing the surface an ocean model (e.g. JPL, Florida State, Perry (2001a,b), O'Brien and Bourassa (2003)). The data sets have been increasing in length with respect to the observation period for several years and now are of reasonable length to assess their use for secondary purposes. Scatterometer data sets give fields of wind vectors which are representative of the wind field close to the ocean's

* Tel.: +1-831-656-3255; fax: +1-831-656-2712.
E-mail address: robint@ucar.edu (R. Tokmakian).

1463-5003/$ - see front matter
doi:10.1016/j.ocemod.2004.04.005

surface (Liu and Katsaros, 2001). Such fields, when translated into fields of wind stress can be used to force the momentum equation at the surface of an ocean model.

Limited studies have been done with these newly created maps of scatterometer wind fields to examine their influence on the circulation fields within an ocean model (e.g. Milliff et al., 1999; Vershell et al., 1999). Milliff et al. (1999) describe the oceanic response in a coarse (about 4°) resolution global model when forced with either a National Centers for Environmental Prediction (NCEP) product or a scatterometer product which repeats annually. They attribute much of the differences in the two simulations to the large scale differences in the mean surface wind fields and not to atmospheric mesoscale features. Additionally, Vershell et al. (1999) describe the results of forcing a 1–1/2 layer, reduced gravity, nonlinear, hydrodynamic tropical model with various wind products and conclude that the scatterometer winds quantitatively improve the representation of the sea level in the tropical Pacific.

The research discussed here takes the use of scatterometer winds a step further by applying the winds to a high resolution, primitive equation ocean model to evaluate the changes in how an ocean model responds to such forcing. The paper presents the results of analyses performed on the output of two ocean simulations which are forced, respectively, with a wind field from the output of the European Centre for Medium Weather Forecasting (ECMWF) meteorological model and with a field created from the wind vectors that are measured by the National Aeronautics and Space Administration (NASA) Quikscat instrument. First, a description of the 0.1° resolution, primitive equation model is given, followed by a section describing the wind field and how the stress field was created to drive the ocean model. Next, the analyses are described which include comparisons to in situ and satellite measurements. This section is followed by a summary of the results with some final thoughts about the use of the scatterometer fields in studies of the ocean's circulation field at various frequencies and wavelengths.

2. Description of the ocean model and forcing fields

The ocean model whose variability is examined in this paper is the Parallel Ocean Program (POP) model (Dukowicz and Smith, 1994). It has a resolution of 0.1° at the equator with 40 levels. It is configured for the North Atlantic basin; the domain is defined as 20°S to 72°N and 98°W to 17°E which includes the Gulf of Mexico and the western Mediterranean Sea. It uses a Mercator grid resulting in horizontal resolutions varying from 11.1 km at the equator to 3.2 km at the northern boundary. The horizontal spacing of this grid is less than or equal to the first baroclinic Rossby radius which results in eddies being reasonably well resolved up to approximately 50° latitude (Smith et al., 2000, Fig. 1). POP has an implicit free surface and includes mixed layer dynamics. The Large et al. (1994) mixed layer formulation, K-Profile Parameterization (KPP), is active in the simulations. The simulations were initialized from previously spun-up simulations. The output of the simulations was saved daily. The analysis uses 2 years, 2000 and 2001.

Two simulations are used in the analyses that follow. The first simulation was forced with daily varying wind stresses derived from the ECMWF (1.25° grid) analysis product for the years spanning 1999 through 2001 (ECMWF run). The second simulation (SCAT run) was forced with a product that used the daily gridded wind vectors provided by the NASA Pathfinder (Perry, 2001a) measured by the Quikscat satellite scatterometer instrument (0.25° grid). Because of the

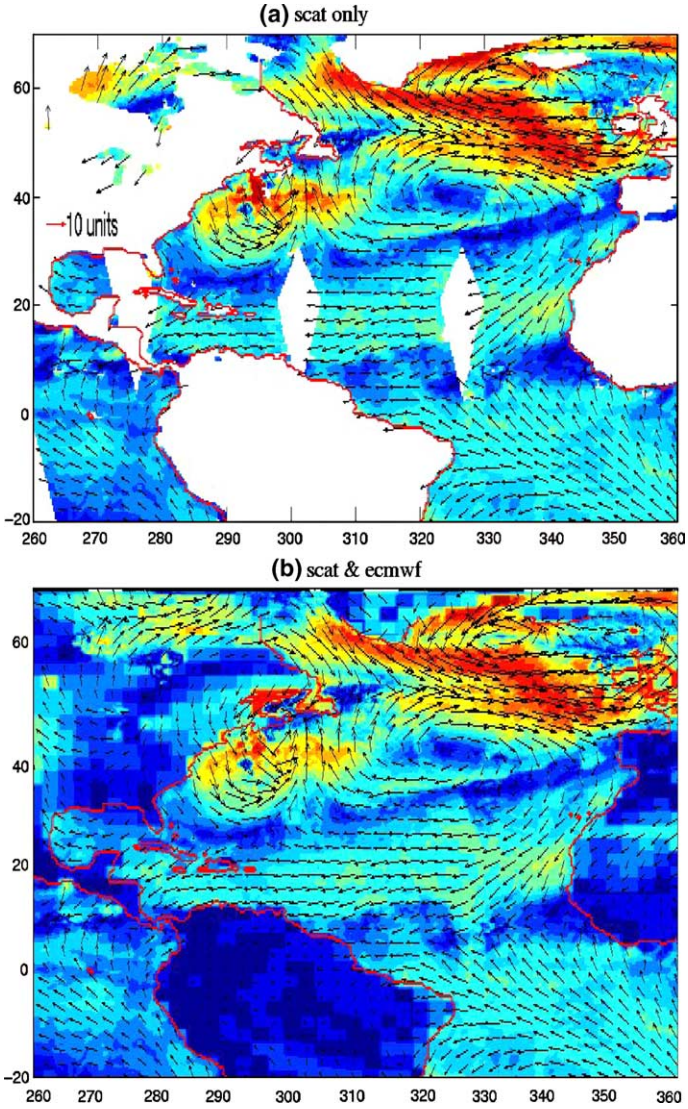

Fig. 1. (a) Daily example of a scatterometer field with amplitude in color overlayed with directional arrows. (b) Same figure except with the holes filled in with ECMWF.

sampling of the earth's surface by the satellite, small holes exist in the gridded product each day. These holes migrate daily around the global grid. Thus, some pre-processing of the wind field is required to produce a complete field to force the ocean model. Various methods were tried to produce a realistic field and in the end, the holes were filled with fields from the ECMWF product from the same time and smoothed to transition from one product to the other. Fig. 1 shows an example of the original field (a) and (b) shows the holes filled with the vectors from the ECMWF product. It is easily seen that the holes of the original product are relatively small (approximately 2° wide and 20° long) and at latitudes between about 10° and 30°N. The holes migrate from day to

day and therefore, the mesoscale structures in the wind fields are compromised only slightly. And as later seen in Section 3, the oceanic response between the two simulations is similar in this region and so any concern that this blending of products is not a primary concern for this application. It should also be noted that the ECMWF product includes the assimilation of scatterometer data from the ERS satellites. These scatterometers sample the ocean differently than the Quikscat data but contribute to the accuracy of the wind vectors in the ECMWF product. It should be noted, though, that this study is primarily addressing the difference in the resolution of the wind field that is forcing the high resolution ocean model.

3. Analyses

3.1. Mean gulf stream path

The mean path of the Gulf Stream Extension is shown as an example of the mean field of the two simulation runs. Fig. 2 shows a random surface temperature field retrieved from NOAAs public web site which is overlaid with two sets of lines. The first set, the solid black lines, representing the mean path (average from 2000/2001) from the ECMWF run and the second set of dotted lines representing the path from the SCAT run are quite similar. The SCAT run is broader in its path than is the ECMWF simulation. The bends and turns of the extension diverge towards

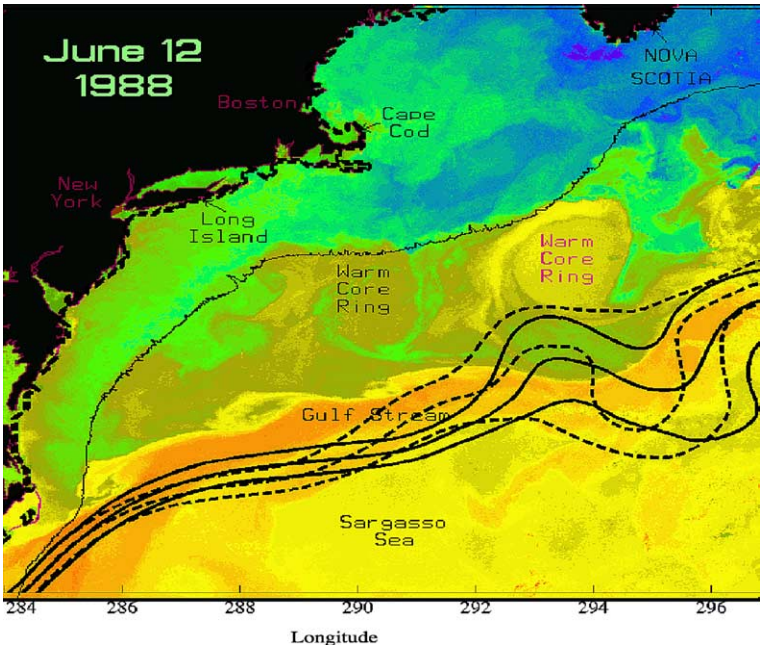

Fig. 2. Random observed ocean temperature field is overlaid with the contours of the mean path of the Gulf Stream Extension. The solid, heavy black line is the contour for the SSH zero line from the ECWMF simulation, while the dashed line is from the SCAT run. For comparison purposes, the path is defined as the zero SSH contour ±20 cm.

the eastern edge of the figure. The mean of the two runs are similar throughout with the differences in the path observed in daily snapshots in the small scale (wavelengths < 200 km) details. These shorter scales are examined in further details in Section 3.4.

3.2. Comparisons to tide gauges

The first, and most robust set used for evaluation is the tide gauge data set from the University of Hawaii (Kilonsky and Caldwell, 1991). A large number of time series from coastal stations in this data set are synoptic with the simulations over the entire period of the simulation. Daily averages of the sea level data set are used for comparisons to the model's sea level anomaly (SLA) field. The tide gauge daily values are compared directly with the SLA at the time of the model's daily average. Previous papers (e.g. Tokmakian and McClean, 2003) have shown that these types of primitive equation ocean models do well at reproducing the variability of the SLA field with respect to the signal observed by tide gauges. In this paper, we are evaluating whether or not the densely sampled scatterometer fields used to force the ocean improves the SLA signal in the model compared to the SLA signal that is produced from using a wind field from a meteorological model (at 1.25° resolution).

Fig. 3 shows the comparison of the correlations between the two simulations' SLA values and the SLA as measured from the tide gauges. In all locations, except for four, the correlations have improved for the simulation forced with scattermeter fields. Of the 39 stations compared, 22 have

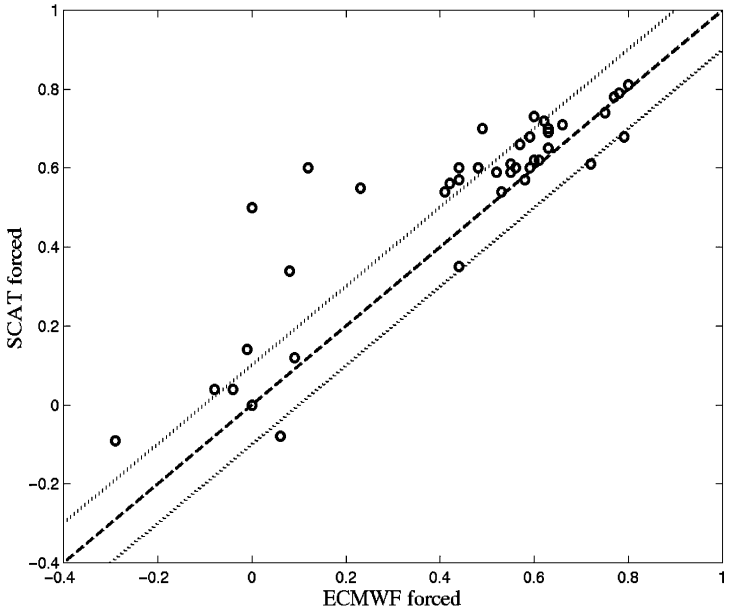

Fig. 3. Correlations between daily tide gauge measurement and ECMWF SLA simulation (x-axis) and scatteromter SLA simulation (y-axis). Dotted lines denote 10% difference line between the two correlation sets. Dashed line denotes the line corresponding to identical values. The bottom axis references the correlations when the model is forced with ECMWF winds and along the vertical axis, the correlation values when the model is forced with the scatterometer winds.

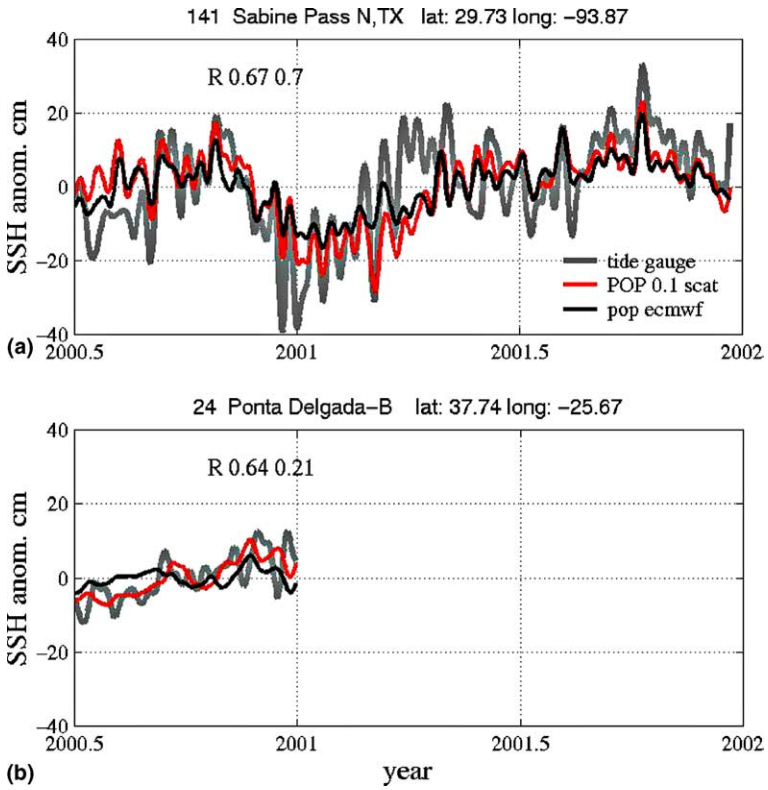

Fig. 4. Time series of tide gauge SLA in gray, scatterometer run SLA in red and ECMWF run SLA in black for 2 locations (a) Sabine Texas and (b) Ponta Delgada.

a significant correlation (R values) of greater than 0.4 and of these, 10 improved their value by 10% when the scatterometer winds were used. For example, the improvement at Sabine Pass, Texas (Fig. 4a, 29.7°N, 93.9°W, $R = 0.7$: SCAT and $R = 0.6$: ECMWF) shows that most of the improvement is in the amplitude of the signal, rather than in the phasing. Both simulations miss the large increase in amplitude in the tide gauge signal around March of 2001, perhaps related to a remotely forced event, not represented in the simulation. At Ponta Delgada ($R = 0.6$ and 0.1, location = 37.7°N, 25.7°W, Fig. 4b), the improvement is in the long period trend of the single.

In summary, to a large extent, the use of a wind field derived from scatterometer measurements from space increased the correlations of the model's SLA to the tide gauge stations slightly. This is not surprising, since the model when driven with the lower resolution ECMWF winds produces realistic variability and in these relatively shallow coastal regions, it reflects, largely, the locally wind driven response.

3.3. Basin-wide SLA signals

To ease the analyses and processing of the various fields compared in this section, the model fields originally on a 0.1° grid are averaged onto a grid at 1°. The observational SLA field used for

comparison is the French product "Maps of Sea Level Anomalies" (MSLA) produced by the AVISO group at CNES (Ducet et al., 2000). The standard processing has been applied to the altimeter data and the data from a set of satellites have been merged and gridded into seven-day maps at the resolution of 0.25°. The data comes from the TOPEX/Poseidon, Geosat Follow-On (GFO), and the multiple European Remote Sensing (ERS) satellites. As a further step, to ease the processing and display of the analyses, the data has been further averaged to a grid of 1°.

Fig. 5a shows a map of the correlations in SLA between the simulation forced with the ECMWF winds and the one forced with scatterometer winds. At low latitudes, the correlations between the SLA responses of the two ocean simulations are somewhat similar except in an area south of about 5°S. Likewise, in the coastal regions, which are the shallower regions of the model, the two wind products produce similar results in the ocean's SLA response, consistent with the results of the tide gauge analysis.

Next, the two model simulations are compared with the gridded field produced from satellite measurements of SLA. The analysis has used the fields gridded at 1°, but for graphing purposes, the results show only at every other grid point. The correlations between the SLA of the scatterometer run and the altimeter data are shown in Fig. 5b, while the Fig. 5c uses the fields of the ECMWF run and the altimeter data. Again similarities in the correlations are extensive between the two simulations. Both simulations show that the ocean response at latitudes below 10° are reasonable. In addition, the mid-latitude areas which show low correlations in (b) and (c) are, in the broad sense, areas that show disagreement in the SLA fields of the two model runs. These are areas of mesoscale activity and the disagreement is indicative of the chaotic and unpredictable nature of the flow. More will be said about this in the next section.

To explore where the impact of using the scatterometer winds is significant, the correlations between the modeled fields and the altimeter fields are used along with a measure of skill for each location. Fig. 6 attempts to give an indication of the regions where the model has some skill in reproducing the ocean's true response to the wind field applied. The dark gray grid points in Fig. 6a are areas where the correlation of the model to the altimeter observations are 0.4 or less and the skill value is less than 10%; meaning that the model is not skillful. The gray areas are regions which have skill in their representation of the true ocean signal and have correlations over 0.4.

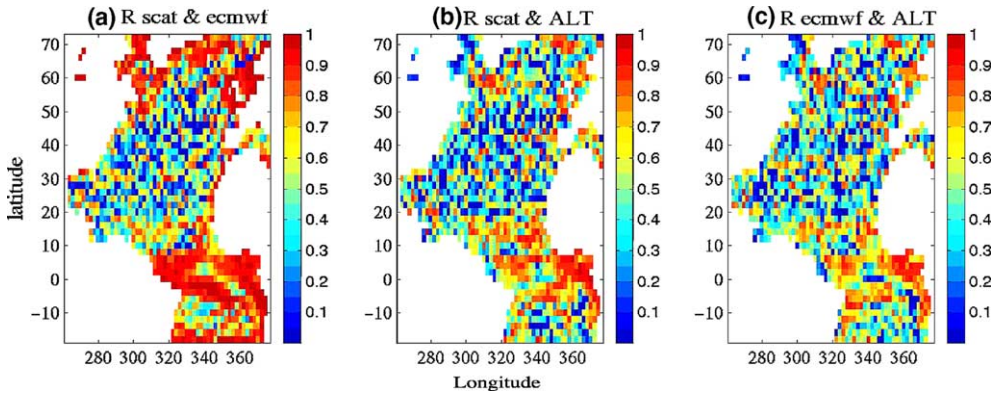

Fig. 5. Correlations of SLA between (a) scatterometer forced simulation and ECMWF forced simulation, (b) scatterometer simulation and altimeter SLA field, and (c) ECMWF simulation and altimeter SLA fields.

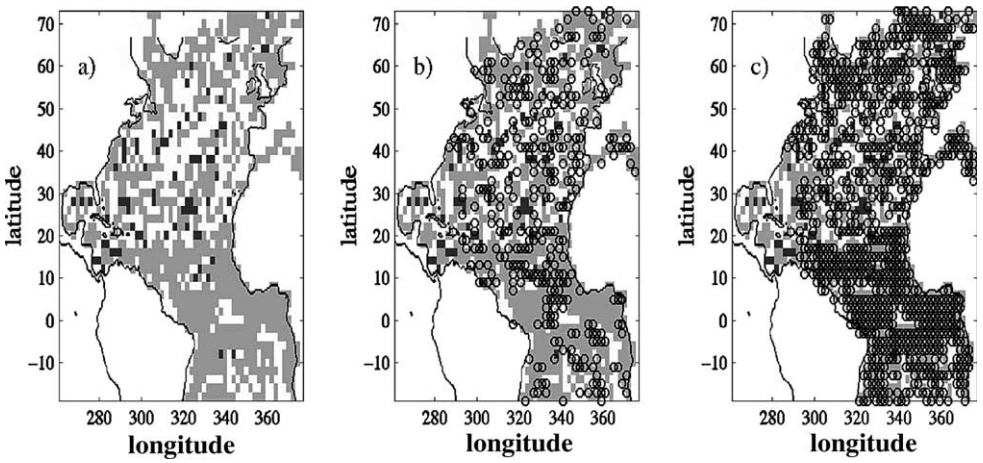

Fig. 6. (a) Map of the model skill of the SCAT run representing the oceanic response of SLA. In both plots, the dark/black areas are low skill areas and the lighter gray shades denote skillful areas. (b) Same as (a) but is overlain with circles which represent grid points where the R value is greater or equal to 0.4 and the SCAT run correlation is 10% greater than the ECMWF run. The right plot (c) is overlain with circles that represent correlations greater than 0.4 for both the ECMWF run and the SCAT run.

And the rest are areas where the signal can not be distinguished from the noise. The circles on Fig. 6b indicate those areas where the correlations in the SCAT run are greater than the correlations of the ECMWF run by at least 10% as well has having values of 0.4 or greater. In Fig. 6c, the circles denote all the points in the SCAT run with skill and significant correlations over 0.4. The regional area that shows consistent improvement with the use of the scatterometer winds is in the eastern tropical Atlantic above the equator centered at 330°E and along 10°N. The mid-latitudes show improvement in the representation of the SSH at points scattered across the mid-latitudes, but not consistent improvement over any wide area. Maps of RMS SSH variability show little systematic improvement in SSH overall. Both wind products produce equal amounts of variability in the SSH which is distributed in time differently in the two runs as seen by the maps of correlations and skill.

3.4. Wave signals

As has been mentioned, the mid-latitudes contain signals that are somewhat chaotic at frequencies of less than a year. Techniques such as radon transforms have been used to examine the wave signal that exists in this frequency band. There have also been many papers written about the planetary wave signal observed in maps of SLA. The analysis presented in this section uses the radon technique that many of these papers have used to explore how planetary waves observed in the altimeter data fit the theoretical values (Chelton and Schlax, 1996; Killworth et al., 1997; Cipollini et al., 1999). The technique is used in this paper to also explore the similarities in the wave energy across a wide range of angles as well as westward planetary wave speeds.

Fig. 7 shows the estimates of the speeds of westward moving waves at various latitudes for the two runs of the model along with the estimates from the altimetric maps. The fields have not been

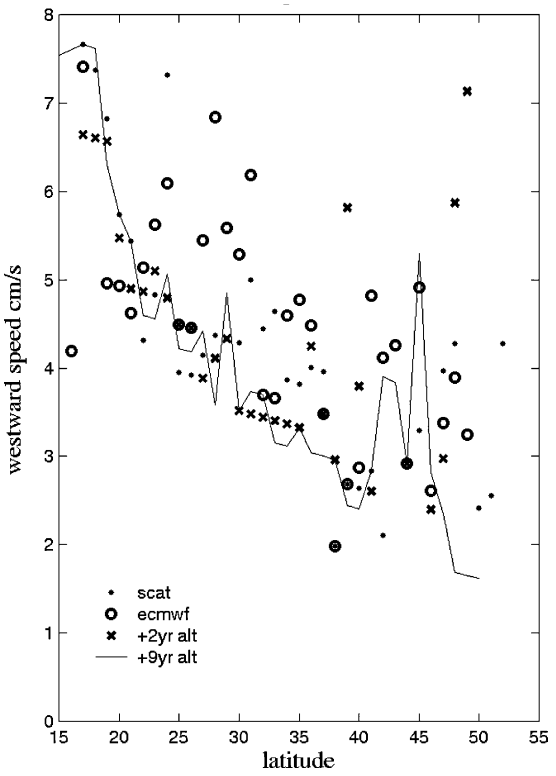

Fig. 7. Estimates of wave speeds: +9 year altimeter estimate—solid line, +2 altimeter estimate—x, +2 year ECMWF run open circles, +2 year SCAT run black dots.

extensively filtered to isolate, specifically, the westward traveling signals as is done by some researchers (e.g. Cipollini et al., 1999). First, it is noted that there are differences at some latitudes (mostly greater than 35° between the +9 year altimetric estimations (solid line) and the +2 year estimates (x's). In addition, the three time series representing a period of +2 year series (black dots—SCAT run, the open circles—ECMWF run, and x's—altimetric data) are also somewhat different. Within the subtropical latitudes (10–30°N) the SCAT run falls close to the speeds as estimated from the altimeter data. Above 30°N, both the SCAT run estimates and the ECMWF run estimates differ from the altimeter estimates, with the SCAT estimates closer to the observed speeds. The ECMWF estimates are generally higher than any of the rest of the estimates.

A measure of how well the model runs reproduce the estimates calculated from the altimetric observations is given by the ratio of the wave speeds from the model runs to the 9 year altimeter data record. At the lower latitudes, the SCAT run generally shows a closer representation of the wave speeds than does the ECMWF run. At the latitudes of 24°N and 32–33°N, the ECMWF run is more realistic, but both have higher speeds than the altimeter time series. A measure of the error of the speed estimates is represented by the RMS difference over the series length in the ratio of the +2 year altimetric series to the +9 year series (solid gray line). Eight of the 21 SCAT estimates are within this band of variability while only five of the twenty ECMWF estimates are within the band. The SCAT ratios not within the band are consistently overestimates of the wave speeds,

while the ECMWF run produces ratios that are both over and underestimates. Thompson et al. (2002) discuss the effects of mixed layer dynamics on the propagation of wind driven planetary waves. The inclusion of a mixed layer with diapycnal mixing inhibits the propagation of planetary waves to some extent. In this study, both simulations include mixing, but to different degrees and this change might explain the difference in the speeds of the planetary waves across the basin.

The energy as represented by the SLA in the two model runs as a function of angle and latitude is shown in Fig. 8a and b, while a similar energy distribution for the +2 year altimeter series is shown in Fig. 8c. Each figure's values are calculated using the radon transform method as applied separately to a time-longitude plot along each zonal line. The result is a plot which shows the relative energy that is propagating at a given angle. The most prominent difference in Fig. 8a and b is between 39 and 42°N, the latitude band of the Gulf Stream (GS) Extension. The SCAT run shows much higher energy levels propagating at all angles than is seen in the ECMWF run. In all three plots, more energy propagates westward than eastward. While the ECMWF forced run

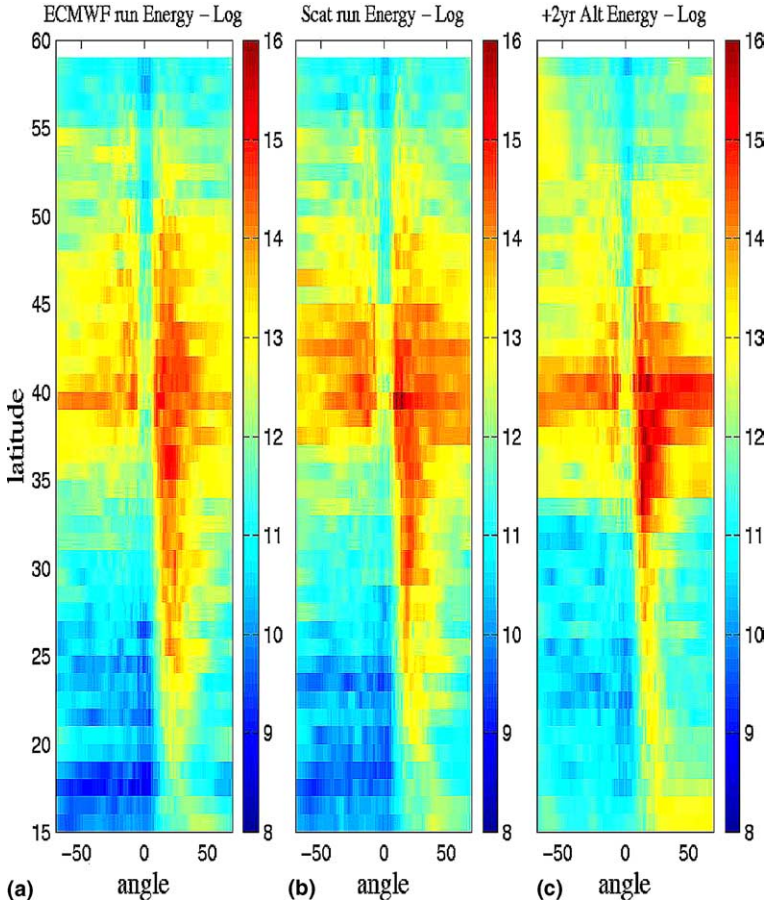

Fig. 8. Wave energy distribution (a) for ECWMF run, (b) for SCAT run, (c) for +2 year altimeter data. Scale is a log scale of arbitrary units. The *x*-axis is the angle along which energy is found to propagate as estimated from a radon transform (where positive angles represent west/northward propagation). The *y*-axis is the latitude.

shows less energy generally than the altimeter data, the SCAT run as a broader distribution of the energy across all angles than seen in the altimeter data. A qualitative assessment of the difference in the two model runs suggests that the SCAT run (Fig. 8b) is the more realistic with a high band of energy distributed across all angles. Another difference is that it would appear that the GS is shifted southward slightly in the SCAT run from what the observations show. This is represented by the region that contains high energy across all bands. This spread of energy is consistent with Fig. 2. It is also noted that in the 15–35°N band, the energy peak in the SCAT run (b) is spread over a wider range of angles, then in the ECMWF run (a).

In summary, the comparison of the SLA field across the basin shows that the use of the scatterometer derived wind stresses produces a better oceanic response than with the use of the ECMWF wind product. The somewhat chaotic planetary wave response appears to be more realistic when forced with SCAT data than with ECMWF fields.

3.5. Mixed layer depth

One of the quantites that is saved during the model runs is the depth of the mixed layer. It is saved on a daily basis. The two simulations, generally, produce similar estimates of the depth of the mixed layer in most regions with the exception of the Labrador Sea, as represented in Fig. 9. Fig. 9a and b represent the mean of the layer's depth for the year 2001 for the SCAT run and ECMWF run, respectively. Fig. 9c is the difference of the two means, while Fig. 9d represents the standard deviation for the period of a year.

The region of the North Atlantic external to the Labrador Sea shows change similar to the area in the plots around 50–52°N with eddy-like signatures. The difference in both the means and their standard deviations indicate that the most intense difference (greater than 100 m) is a relatively small area centered at 310°E, 58°N. Examining the fields at higher resolution does not seem to

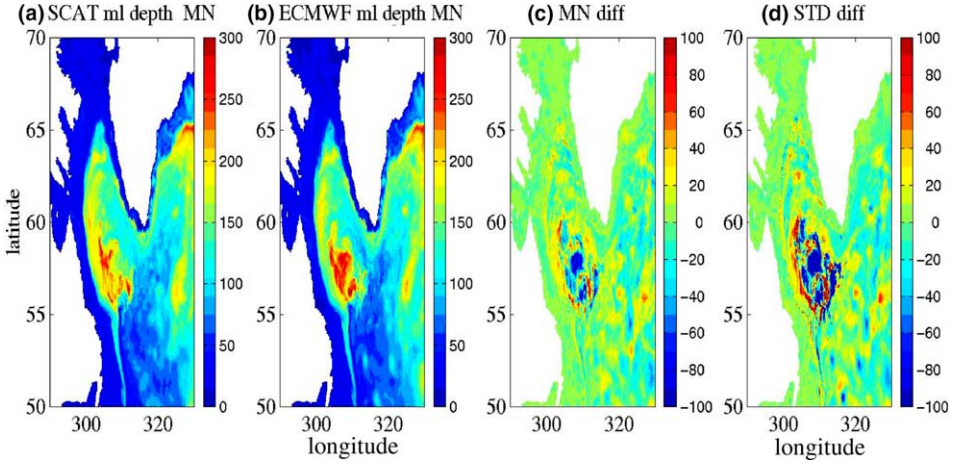

Fig. 9. (a) Mean of scatterometer run mix layer in Labrador Sea, (b) same for ECMWF run, (c) difference in mean, (d) difference in the standard deviation. The sense of the plot is that the blue regions are regions where the depth of the ECMWF run is deeper than that of the SCAT run and the yellow/red regions are where the SCAT run produces deeper depths or larger variances from the mean.

indicate that the small scale structure is more defined in the SCAT run verse that seen in the ECMWF run. The general strength of the wind field is similar in both simulations, but there is a higher spatial variability by about 15% in the scatterometer wind field, resulting in a less coherent wind field across the area.

A set of time series of the mixed layer depth can be extracted from the output fields for the two runs and is shown in Fig. 10. The location is at a point where the deepest mixing is, 58°N, 51°W. It can be seen that for much of the year the values are similar. The winter mixing seen during the February/March time frame is distinctly deeper when the model is forced with the ECMWF product than when forced with the scatterometer winds. In situ station data for the same time period as the simulation has been collected by IMF Kiel (see: http://www.ifm.uni-kiel.de/fb/fb1/po1/research/sfb460/a2/sfb-a2.html) and by examining that data set qualitatively, the observational depths more closely resemble the shallower representation of the mixed layer depth of the run forced with the scatterometer winds. Further examination of the vertical structure in this region shows that the vertical stability (Fig. 11a) of the two simulations is different in the period prior to deep winter mixing. The SCAT run has a slightly more stable structure than does the ECMWF run. Fig. 11b indicates that at the surface, the temperatures are similar as expected from the use of a relaxation term, while at depth, the waters of the SCAT run are cooler than in the ECMWF run. Thus, the waters of the two runs are "pre-conditioned" differently prior to the winter mixing. This difference can be explained be looking at the curl of the wind stress (Fig. 11c) which for the SCAT run is more positive than the ECMWF data for the period between September and December of 2000. This contrasts to the summer/fall of 2001, where the difference in temperature is more easily explained by the passage of an eddy in the SCAT simulation which warms both the shallow and the deeper waters of the SCAT run, but has a similar wind stress applied for the summer period for the two simulations. Therefore, it can be argued that it is the difference in the winds prior to deep winter mixing and their "pre-conditioning" of the deep waters that have led to a difference in the depth of the winter mixed layer.

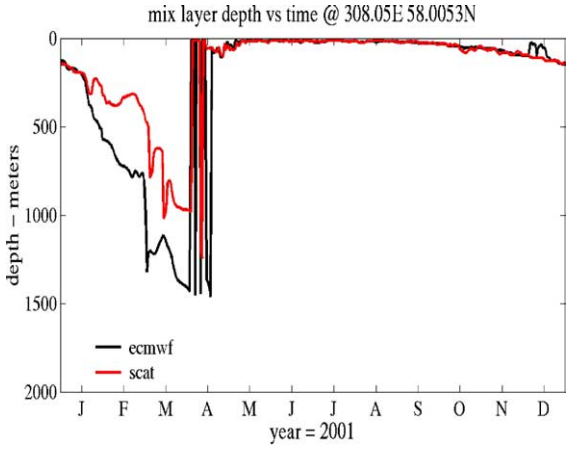

Fig. 10. Time series of the mix layer depth at a location near Ocean Station Bravo and IMF Kiel stations K1-K41, 58°N, 51°W. The SCAT run is shown in red and the ECWMF run is the black line for the year 2001.

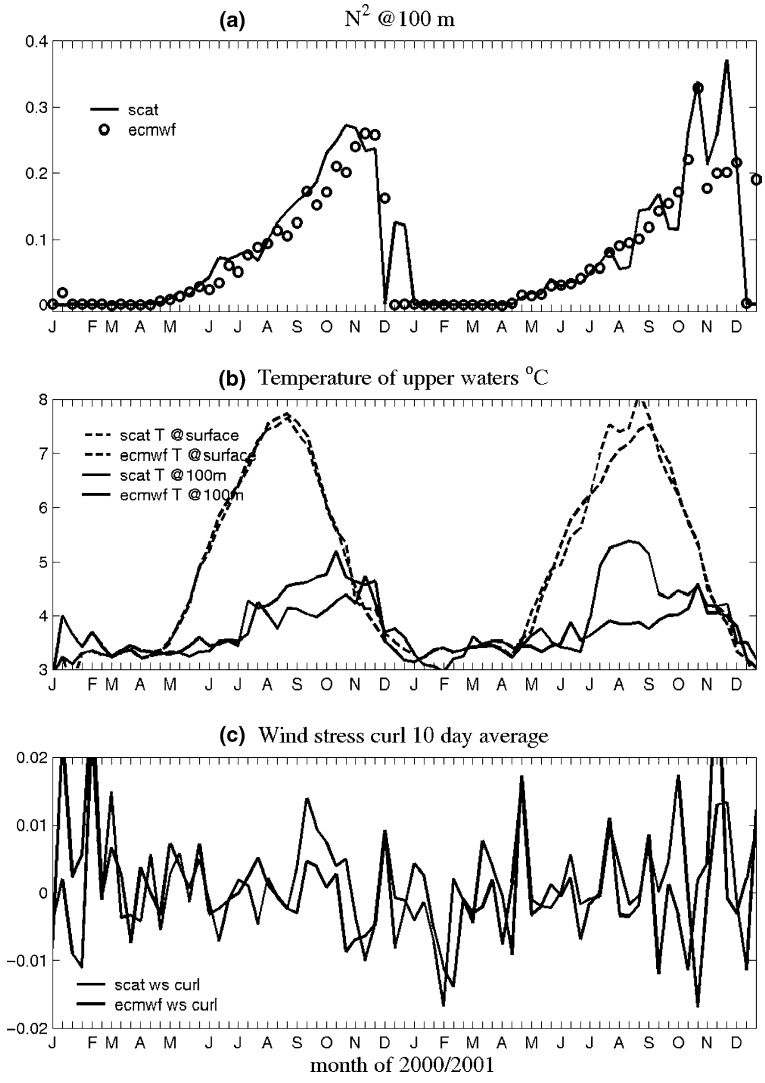

Fig. 11. (a) N2 (Brunt–Visala frequency at 58°N, 51°W. SCAT run (black line), ECMWF run (circles), (b) temperature at surface and at 100 m for SCAT run (gray dashed and solid lines) and ECMWF run (black dashed and solid lines), (c) wind stress curl at 58°N, 51°W for SCAT run (gray line) and ECMWF run (black line).

In the subtropics (15–30°N), the difference in the mean mixed layer depth between the two simulations is about 2 m with a standard deviation of 10 m for the SCAT run and 9 m for the ECMWF run. If a time-latitude plot is made of the mixed layer depth, along with a plot of SLA at 25°N (not shown), interesting similarities and differences are seen. Clear propagating signals can be seen in both the SLA and the MLA. During the winter mixing, differences in the mixed layer depth are due to the strength of the mixing locally. Although the mixed layer differences are relatively small as compared to the Labrador sea, the SCAT run shows stronger mixing, spread over a wider area than is seen in the ECMWF run.

It has been shown how the two simulations differ in their variability of the upper levels of the ocean. Clearly there are connections between the processes of the mixed layer and surface. Whether these differences in the two model runs are important in their connection to ecosystem changes are something that will be investigated at a later date.

4. Conclusions

While previous studies (e.g. Tokmakian, 1996) have shown that the seasonal cycle of the SLA is reasonably reproduced in model simulations, the realism of the higher frequency signals are much more difficult to quantify. From these two simulations, it can be argued that there is improvement in the representation of SLA when the scatterometer winds are used, especially in the tropical band. These results confirm the conclusions of Vershell et al. (1999) that forcing with scatterometer winds produce a quantitative better ocean response. The correlations are relatively lower (along with a lower skill) in the North Atlantic between 10 and 50°N because the mesoscale and high frequency signals of the SLA are somewhat chaotic. With only small differences in the wind fields, significant differences in wave propagation speeds are seen. Whenever possible, scatterometer winds should be used. The limitation in using these data to force ocean hindcast models is the length of the time series which restricts such simulations to a few years. These relatively short simulations can be used in conjunction with those run for longer periods with the reanalysis wind fields (e.g. ERA40, NCEP Reanalyses) to better understand the ocean processes that may be influenced by the finer spatial sampling of the wind field by the scatterometer. This would especially be true when using high resolution ocean models.

Acknowledgements

Support for this research has been provided by NASA, under T/P-Jason SWT. The author thanks JPL for providing the gridded wind fields. Thanks also to the French CNES/AVISO group for their gridded and merged fields of altimeter SLA and the University of Hawaii Sea Level Center for the tide gauge data. The computing resources were provided for by the Dept. of Defense High Performance Computing Modernization Office, ARL, NAVO. My thanks is also extended to the reviewers of this paper for their helpful critique.

References

Chelton, D.B., Schlax, M.G., 1996. Global observation of oceanic Rossby waves. Science 272, 234–238.

Cipollini, P., Cromwell, D., Quartly, G.D., 1999. Observations of rossby wave propagation in the Northeast Atlantic with TOPEX/POSEIDON altimetry. Adv. Space Res. 22, 1553155.

Ducet, N., Le Traon, P.-Y., Reverdin, G., 2000. Global high resolution mapping of ocean circulation from TOPEX/Poseidon and ERS-1 and -2. J. Geophys. Res. 105, 19477–19498.

Dukowicz, J.K., Smith, R.D., 1994. Implicit free-surface method for the Bryan–Cox–Semtner ocean model. J. Geophys. Res. 99, 7801–7991.

Killworth, P.D., Chelton, D.B., de Szoeke, R., 1997. The speed of observed and theoretical long extratropical planetary waves. J. Phys. Oceanogr. 27, 1946–1966.

Kilonsky, B., Caldwell, P., 1991. In the pursuit of high quality SL data. IEEE Oceans Proc. 2, 669–675.

Large, W.G., McWilliams, J.C., Doney, S.C., 1994. Oceanic vertical mixing: a review and a model with a nonlocal boundary layer parameterization. Rev. Geophys. 32, 363–403.

Liu, W.T., Katsaros, K.B., 2001. Air-sea flux from satellite data. In: Siedler, G., Church, J., Gould, J. (Eds.), Ocean Circulation and Climate. Academic Press, New York, pp. 173–1179.

Milliff, R.F., Large, W.G., Morzel, J., Danabasoglu, G., Chin, T., 1999. Ocean general circulation model sensitivity to forcing from scatterometer winds. J. Geophys. Res., 11337–11358.

O'Brien, J.J., Bourassa, M.A., 2003. The best winds for ocean models?, AMS Annual Conference.

Perry, L., 2001a. (Ed.), QuikSCAT Science Data Product Users Manual, Jet Propulsion Laboratory, document number D-18053, p. 86.

Perry, K.L., 2001b. SeaWinds on QuikSCAT level 3, Daily, Gridded Ocean Wind Vectors (JPL SeaWinds Project) Guide Document Version 1.1 D-20335, JPL, Pasadena, CA.

Smith, R.D., Maltrud, M.E., Bryan, R.O., Hecht, M.W., 2000. Numerical simulation of the North Atlantic ocean at 1/10°. J. Phys. Oceanogr. 30, 1532–1561.

Thompson, L., Kelly, K.A., Darr, D., Hallberg, R., 2002. Buoyancy and mixed-layer effects on the sea surface height response in an isopycnal model of the North Pacific. J. Phys. Oceanogr. 32, 3657–3670.

Tokmakian, R.T., 1996. Comparisons of time series from two global models with tide gauge data. Geophys. Res. Lett. 23, 3759–3762.

Tokmakian, R., McClean, J.L., 2003. How realistic is the high frequency signal of a 0.1-degree resolution ocean model?, J. Geophys. Res., 108, 3115, doi:10.1029/2002JC001446.

Vershell, M.A., Bourassa, M.A., Weissman, D.E., O'Brien, J.J., 1999. Ocean model validation of the NASA scatterometer winds. J. Geophys. Res. 104, 11359–11373.